THE JOURNAL OF BIOLOGICAL CHEMISTRY
Vol. 279, No. 10, Issue of March 5, pp. 9298–9305, 2004
Printed in U.S.A.

The Intracellular Chloride Ion Channel Protein CLIC1 Undergoes a Redox-controlled Structural Transition*

Received for publication, August 1, 2003, and in revised form, October 15, 2003
Published, JBC Papers in Press, November 12, 2003, DOI 10.1074/jbc.M308444200

Dene R. Littler‡§¶, Stephen J. Harrop‡§¶, W. Douglas Fairlie§¶‖, Louise J. Brown‡§, Greg J. Pankhurst§, Susan Pankhurst§, Matthew Z. DeMaere‡, Terence J. Campbell, Asne R. Bauskin§, Raffaella Tonini‡‡, Michele Mazzanti‡‡, Samuel N. Breit§¶, and Paul M. G. Curmi‡§¶**

*From the ‡Initiative for Biomolecular Structure, School of Physics, University of New South Wales, Sydney, New South Wales 2052, Australia, §Centre for Immunology, St. Vincent's Hospital and University of New South Wales, Sydney, New South Wales 2010, Australia, **Department of Medicine, University of New South Wales, Sydney, New South Wales 2052, and ‡‡Department of Cellular and Developmental Biology, University of Rome "La Sapienza," 00185 Rome, Italy*

Most proteins adopt a well defined three-dimensional structure; however, it is increasingly recognized that some proteins can exist with at least two stable conformations. Recently, a class of intracellular chloride ion channel proteins (CLICs) has been shown to exist in both soluble and integral membrane forms. The structure of the soluble form of CLIC1 is typical of a soluble glutathione *S*-transferase superfamily protein but contains a glutaredoxin-like active site. In this study we show that on oxidation CLIC1 undergoes a reversible transition from a monomeric to a non-covalent dimeric state due to the formation of an intramolecular disulfide bond (Cys-24–Cys-59). We have determined the crystal structure of this oxidized state and show that a major structural transition has occurred, exposing a large hydrophobic surface, which forms the dimer interface. The oxidized CLIC1 dimer maintains its ability to form chloride ion channels in artificial bilayers and vesicles, whereas a reducing environment prevents the formation of ion channels by CLIC1. Mutational studies show that both Cys-24 and Cys-59 are required for channel activity.

Chloride ion channels control a variety of cellular processes that are central to normal function and disease states (1). The CLIC[1] family is a recently identified class of Cl^- channel proteins that consists of seven members (p64, parchorin, CLIC1–5) (2, 3). A conserved C-terminal CLIC module of ~240 amino acids is present in each member of the family with several members containing additional, unrelated N-terminal domains. Most CLICs are localized to intracellular membranes and have been linked to functions including apoptosis, pH, and cell cycle regulation (4–6). The CLIC ion channels are unusual in that they possess both soluble and integral membrane forms (2). In this regard they are similar to some bacterial toxins and several classes of intracellular proteins including Bcl-x_L and the annexins (7). Our understanding of how such dual natured proteins enter the membrane is limited by the dearth of high resolution structures for key states in this process.

We have recently determined the crystal structure of a soluble monomeric form of CLIC1 (8) and found that it is a structural homologue of the GST superfamily of proteins (9). This soluble form of CLIC1 consists of two domains, the N-domain possessing a thioredoxin fold closely resembling glutaredoxin and an all α-helical C-domain, which is typical of the GST superfamily. CLIC1 contains an intact glutathione-binding site that was shown to covalently bind glutathione via a conserved CLIC cysteine residue, Cys-24. This led to the suggestion that CLIC1 function may be under redox control, possibly via reactive oxygen or nitrogen species.

The structure and stoichiometry of the integral membrane form of the CLIC proteins is still unclear. Electrophysiology of purified, soluble (*Escherichia coli*-expressed) recombinant CLIC1 in reconstituted artificial bilayers shows that CLIC1 alone is sufficient for chloride ion channel formation (8, 10–12). Electrophysiological studies of FLAG epitope-tagged CLIC1 in the plasma membranes of Chinese hamster ovary K1 cells suggest an extracellular N terminus and a cytoplasmic C terminus (13). These experiments imply that in the channel form of the protein, CLIC1, crosses the membrane an odd number of times.

One or possibly two putative transmembrane helices have been postulated to form the membrane-spanning region(s) of the CLIC module (2). The most conserved of these putative TM regions (residues 24–46; CLIC1 numbering) is located within the N-terminal domain and contains Cys-24, which is at the center of the glutathione-binding site. In the structure of the monomeric soluble form of CLIC1, this putative N-terminal transmembrane segment forms an α helix (h1) and β-strand (s2) within the glutaredoxin-like N-domain (8). Thus, CLIC1 is

* This work has been funded by National Health and Medical Research Council of Australia, Australian Research Council, University of New South Wales, St. Vincent's Hospital, Meriton Apartments Pty. Ltd. via R&D Syndicate arranged by Macquarie Bank Ltd., New South Wales Health Research and Development Infrastructure, Italian Ministry of University and Research, and "La Sapienza" University. The costs of publication of this article were defrayed in part by the payment of page charges. This article must therefore be hereby marked "*advertisement*" in accordance with 18 U.S.C. Section 1734 solely to indicate this fact.

The atomic coordinates and structure factors (code 1RK4) have been deposited in the Protein Data Bank, Research Collaboratory for Structural Bioinformatics, Rutgers University, New Brunswick, NJ (http://www.rcsb.org/).

¶ These authors contributed equally to this work.

‖ Present address: Walter and Eliza Hall Institute of Medical Research, Royal Parade, Victoria 3050, Australia.

§§‖ To whom correspondence should be addressed: School of Physics, University of New South Wales, Sydney NSW 2052, Australia. Tel.: 61-2-9385-4552; Fax: 61-2-9385-6060 E-mail: p.curmi@unsw.edu.au.

[1] The abbreviations used are: CLIC, chloride intracellular ion channel; GST, glutathione *S*-transferase; DTT, dithiothreitol.

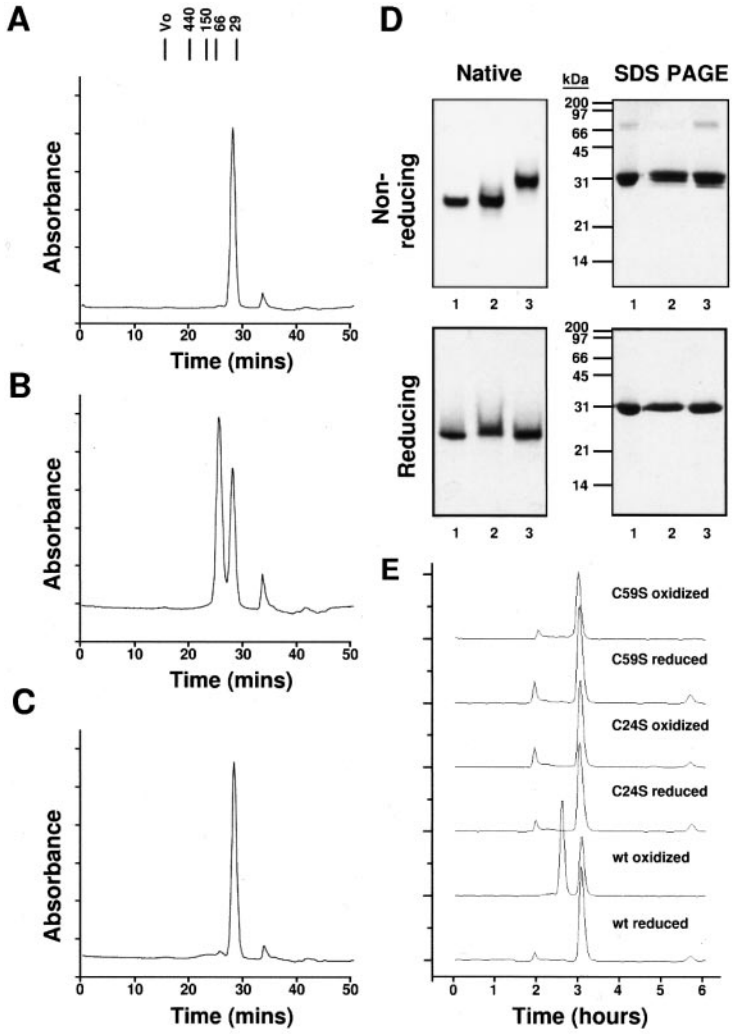

FIG. 1. **Biochemical analysis of the oxidized CLIC1 dimer.** Gel filtration chromatography of CLIC1 using a Superose 12 (HR 10/30) column is shown. *A*, before oxidation. *B*, after oxidation by 2 mM H_2O_2 for 1 h at room temperature. *C*, after subsequent reduction by 50 mM DTT for 1 h at room temperature. The abscissae give the absorbance at 280 nm. *D*, electrophoretic analysis of CLIC1, where *lane 1* shows untreated CLIC1, whereas *lanes 2* and 3 show the monomer and dimer peak fractions after oxidation (as per *B*). The *left panels* show 10% native gels, whereas the *right panels* show 15% SDS-PAGE gels run under both non-reducing (*upper panels*) and reducing (*lower panels*) conditions. *E*, gel filtration chromatography of CLIC1 mutant proteins using a Superdex G75 preparative column (HiLoad 26/60, Amersham Biosciences). The series of chromatograms show wild-type (*wt*), C24S, and C59S CLIC1 under reducing conditions and after oxidation via the addition of 2 mM H_2O_2 for 2 min at room temperature.

likely to undergo a large scale structural rearrangement on transiting to the integral membrane form. This structural change may involve the N-domain of CLIC1 and, hence, disrupt the glutathione-binding site. We note that this transmembrane segment is only putative, and other hypotheses exist as to how CLIC1 is transformed into an integral membrane ion channel protein (11).

In this paper we examine the effect of oxidation on the structure of CLIC1. Incubation with H_2O_2 results in the formation of an intramolecular disulfide bond and non-covalent dimerization. This transition is reversible on reduction. We present the crystal structure of this soluble, oxidized dimeric form of CLIC1 at 1.8-Å resolution. The structure is markedly different from the soluble, monomeric form in that the glutaredoxin-like N-domain has undergone a radical rearrangement to expose an extended hydrophobic surface, which forms the dimer interface. This transition is stabilized through the formation of an intramolecular disulfide bond between two originally distant cysteine residues, Cys-24 and Cys-59. The dimer forms chloride ion channels in artificial lipid bilayers that are similar to the native channel. Finally, we show that purified CLIC1 cannot form ion channels in lipid bilayers under reducing conditions and that mutation of either Cys-24 or Cys-59 to serine results in the loss of channel activity.

EXPERIMENTAL PROCEDURES

Expression, Purification, and Oxidation of CLIC1—Recombinant GST-CLIC1 fusion proteins (wild type and mutants) were expressed in *E. coli* BL21(DE3)pLysS using the pGEX-4T-1 vector (2). The fusion protein was purified from the cell lysis supernatant by binding to glutathione S-Sepharose (Amersham Biosciences) and cleaved using bovine plasma thrombin (Sigma). Protein was further purified at 4 °C by gel filtration on a Superdex G75 column (Amersham Biosciences) preequilibrated with 10 mM Hepes, 100 mM KCl, 0.5 mM $CaCl_2$, 1 mM DTT, and 1 mM NaN_3 at pH 7.0. The resulting peak at 30 kDa corresponding to monomeric CLIC1 was dialyzed at 4 °C into 1× phosphate-buffered saline and concentrated to 15 mg/ml. The final product consisted of the wild-type CLIC1 sequence with an extra two residues at the N terminus (Gly-Ser) as a result of the thrombin cleavage site in the fusion construct.

Oxidation Experiments—To examine the effect of hydrogen peroxide treatment on CLIC1, a 20 mM stock solution of hydrogen peroxide was prepared immediately before use then added at a final concentration of 2 mM to typically 20–50 μl of the purified protein (~2 mg/ml) in 20 mM potassium phosphate buffer, pH 7.0, containing 150 mM NaCl and incubated for various time periods at room temperature. After incubation the proteins were either analyzed directly by gel filtration chromatography as described below or reduced by the addition of DTT to a final concentration of 50 mM and incubated for a further 1 h at room temperature before gel filtration.

For gel filtration chromatography analysis untreated and oxidized proteins were diluted to 200 μl final volume before injection onto a Superose 12 (HR 10/30, Amersham Biosciences) column preequilibrated in phosphate-buffered saline, pH 7.4, at 0.5 ml/min. Proteins were detected by absorbance at 280 nm. The column was calibrated with the standard proteins carbonic anhydrase (29 kDa), bovine serum albumin (66 kDa), yeast alcohol dehydrogenase (150 kDa), β-amylase (200 kDa), ferritin (440 kDa), and the column void volume was determined from the elution time of blue dextran (2×10^6 kDa).

Electrophoresis was performed either under non-denaturing conditions using 10% native polyacrylamide gels or under denaturing

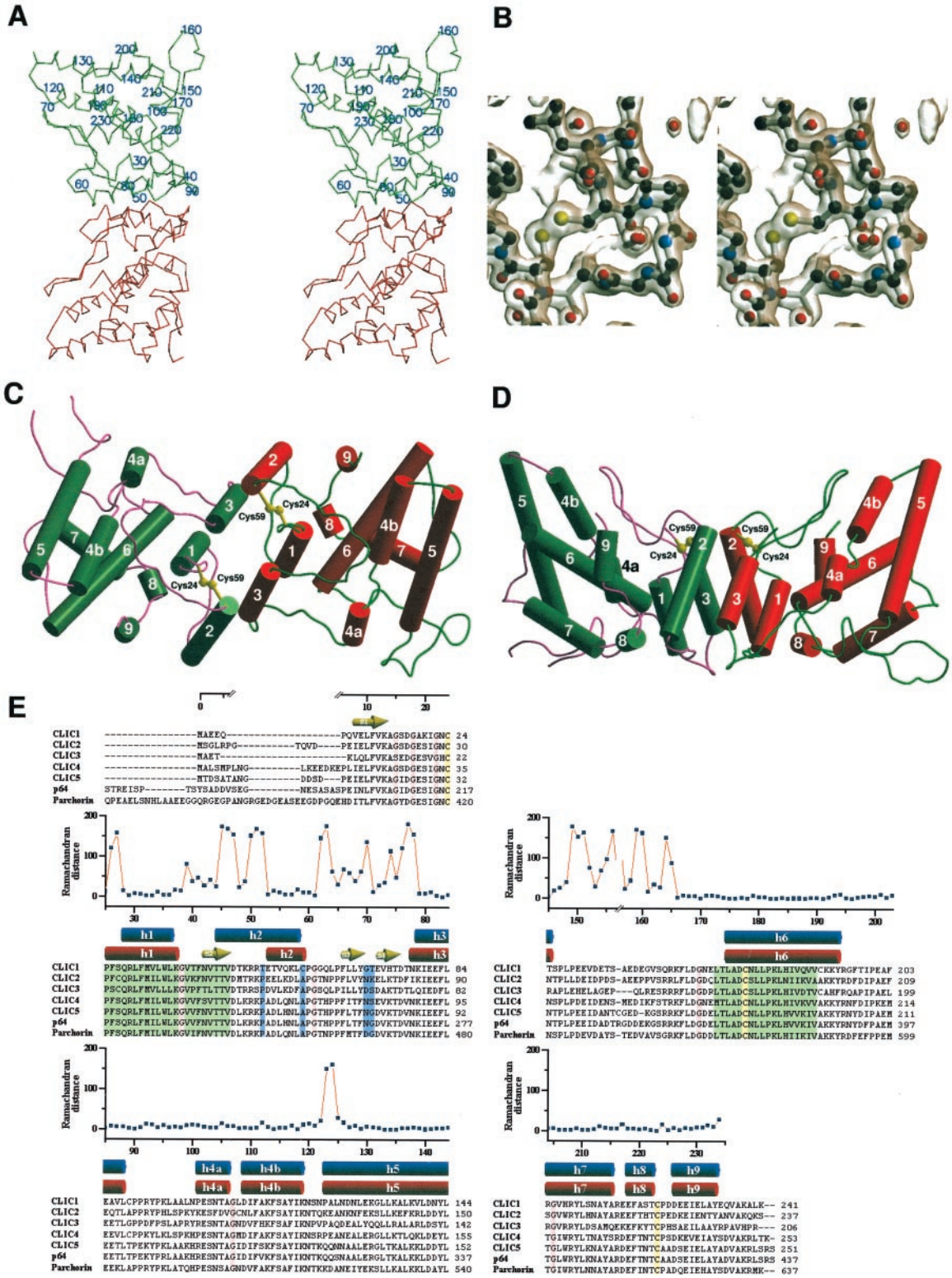

FIG. 2. **Structure of the oxidized CLIC1 dimer.** *A*, stereo backbone of the CLIC1 dimer; *green*, A subunit; *red*, B subunit. In the A subunit every 10th residue is labeled. *B*, electron density of the intramolecular disulfide bond between Cys-24 and Cys-59 contoured at 1σ. The CLIC1 dimer is viewed along (*C*) and perpendicular (*D*) to the pseudo 2-fold axis; are shown helices, A subunit (*red*) and B subunit (*green*), and intramolecular disulfide bonds (*yellow*). *E*, ClustalW (24) alignment of the CLIC family. The secondary structure is shown for both monomeric (*red*, helices; *yellow*, β-strands) and dimeric (*blue*, helices) forms. Conserved regions are *shaded*; *green*, putative transmembrane regions; *yellow*, Cys; *cream*, Gly. Features unique to CLIC1 are in *blue*. Ramachandran distances (see "Experimental Procedures") for the monomer to dimer transition are plotted above its sequence. Figures were made with SETOR (25), MOLSCRIPT (26), RASTER3D (27), and CONSCRIPT (28).

conditions by SDS-PAGE on 15% gels. Samples were electrophoresed either unreduced or reduced by the addition of 50 mM DTT to the sample buffer. Bands were visualized by Coomassie Brilliant Blue staining.

Crystallization of the Oxidized CLIC1 Dimer—CLIC1 was oxidized by the addition of H_2O_2 to a final concentration of 2 mM in phosphate-buffered saline solution. The protein was incubated under oxidizing conditions for 5 min at 18 °C before dialyzing against 10 mM Hepes, 100

mM KCl, 0.5 mM $CaCl_2$, and 1 mM NaN_3 at pH 7.0 for 2 h at 4 °C and purified on a Superdex G75 column preequilibrated in the same buffer. Protein eluted as two peaks corresponding to dimeric (60 kDa) and monomeric (30 kDa) CLIC1. The dimeric fraction was passed over the Superdex G75 column a second time, and the resulting single 60kDa peak was concentrated, flash-frozen in liquid nitrogen, and stored at −80 °C.

Crystals were obtained at 4 °C by sitting drop vapor diffusion with 5 μl of protein (7.6 mg ml^{-1}) plus 5 μl of reservoir solution (14% w/v polyethylene glycol monomethyl ether 5000 (Hampton Research), 0.1 M sodium acetate, pH 4.5). Crystals were flash-frozen in liquid nitrogen after a serial transfer into cryoprotectant consisting of reservoir solution plus 10% v/v polyethylene glycol 400 and 300 mg ml^{-1} D-glucose (ICN Biomedicals). Diffraction data were obtained at 100 K on a DIP2030 imaging plate mounted on a Nonius rotating anode generator using copper Cu K_α radiation and focusing mirrors. The crystals diffracted to 1.8 Å resolution in the space group $P2_12_12_1$ (a = 59.91 Å, b = 69.23 Å, c = 107.51 Å).

TABLE I
Data reduction and refinement statistics
r.m.s.d., root mean square deviation.

Reflections (unique)	163,232 (40,808)
Completeness (1.86-1.8Å shell)	95.3 % (85.1%)
I/σ (1.86–1.8-Å shell)	10.7 (2.8)
R_{merge} (1.86–1.8-Å shell)	0.058 (0.26)
Protein (water) atoms	3346 (268)
R factor (R_{free})	0.196 (0.228)
r.m.s.d. bond lengths[a]	0.011 Å
r.m.s.d. bond angles[a]	1.44°
Ramachandran plot[a]	
Most favored region	94.1%
Additionally allowed	5.6%
Disallowed	0.3 % (Ala-125, A subunit)

[a] From Procheck (31).

Structure Determination and Refinement—Data were processed with the programs MOSFLM (14) and SCALA (15). The CLIC1 monomer structure (1K0M) (8) was used as a molecular replacement probe using the CCP4 (15) program AmoRe (16). An initial phasing model consisting of two C-terminal domains (residues 92–241) was used in the program wARP (17) for phase refinement. The resulting electron density map was clear, and a model was built using the program O (18). This was refined using maximum likelihood methods (program REFMAC V (19)). The final model consists of residues 23–234 in the A subunit and residues 23–154 and 158–234 in the B subunit plus 268 water molecules. The final R-factor is 0.196 with R-free at 0.228. The data reduction and refinement statistics are summarized in Table I.

Ramachandran Distance—We compared the Ramachandran plots of CLIC1 in the monomeric and dimeric states and computed a Ramachandran distance (degrees), D, for residues 24–233 as,

$$D = \sqrt{(\phi_D - \phi_M)^2 + (\psi_D - \psi_M)^2} \quad \text{(Eq. 1)}$$

where subscripts D and M refer to the dimer and monomer structures.

Chloride Efflux Experiments—400-nm unilamellar liposomes (soybean phosphatidylcholine:cholesterol 9:1 w:w; Sigma P-5638 and C-8662, respectively) containing 200 mM KCl, 2 mM HEPES, pH 6.5, were prepared by extrusion (Avestin Lipofast extruder) and extravesicular chloride removed by desalting on Bio-Gel P-6DG spin columns (Bio-Rad) equilibrated in "assay buffer" (330 mM sucrose, 2 mM HEPES, pH 6.5). A chloride selective electrode (Radiometer Pacific) was used to monitor chloride efflux from the vesicles upon the addition of freshly prepared CLIC1 equilibrated in assay buffer. In each experiment protein (30 μg/ml final concentration) was added to the liposomes followed by 3 μM valinomycin to initiate potential driven

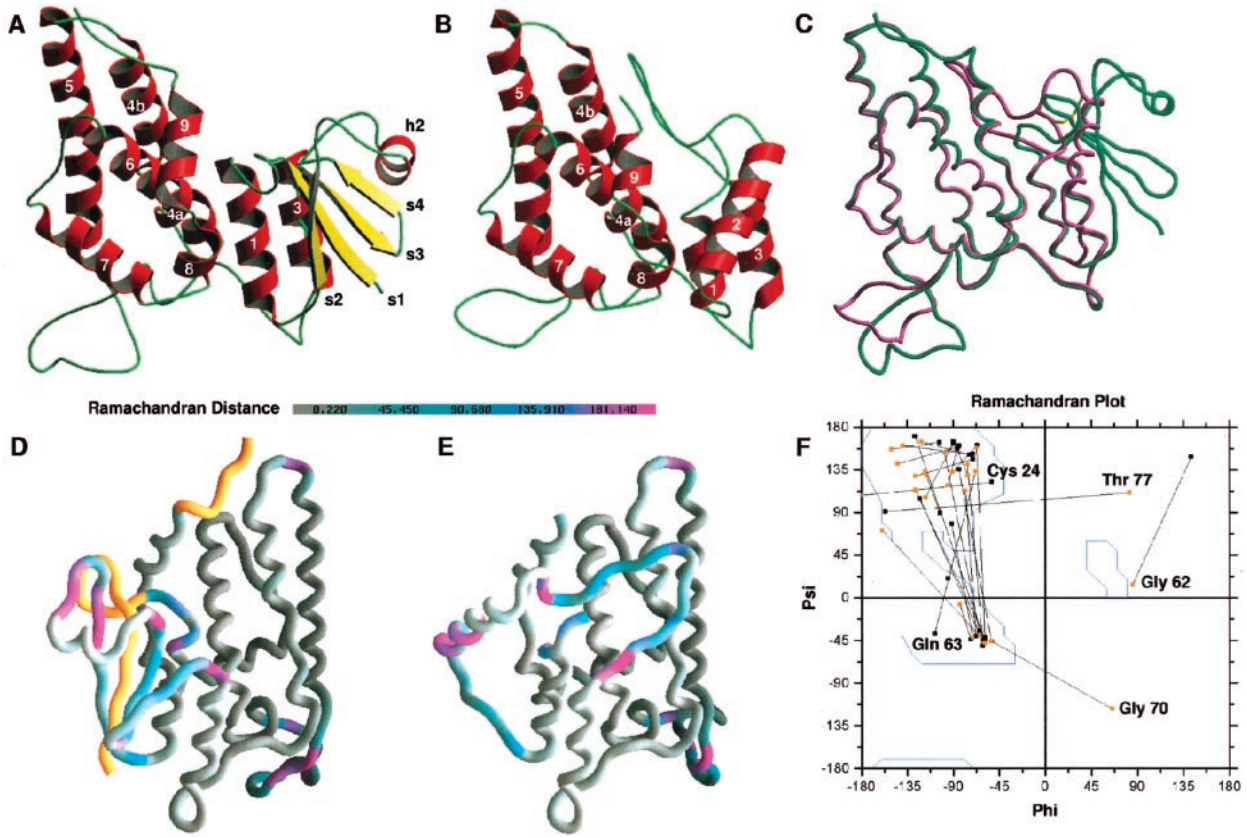

FIG. 3. **Structural transition of CLIC1 between the monomeric and the dimeric forms.** Representations of reduced monomeric form of CLIC1 (*A*) and a subunit of the oxidized dimeric form (*B*). *C*, backbone superposition of CLIC1 for the reduced monomeric (*green*) and the oxidized dimeric (*magenta*) states. Ramachandran distances for residues 23–234 are mapped onto the backbone of the monomeric (*D*) and dimeric (*E*) forms. The color gradient, from *gray* to *pink* represents Ramachandran distances from 0° to 180°. Residues not observed in the dimer are colored *gold*. *F*, Ramachandran plot of residues within the N-domain with Ramachandran distances greater than 35^0 between the two structures. Monomer ϕ-ψ co-ordinates are plotted as *orange squares*, and dimer co-ordinates are in *black* with a connecting line. The figures were made with SETOR (25), MOLSCRIPT (26), RASTER3D (27), and GRASP (29).

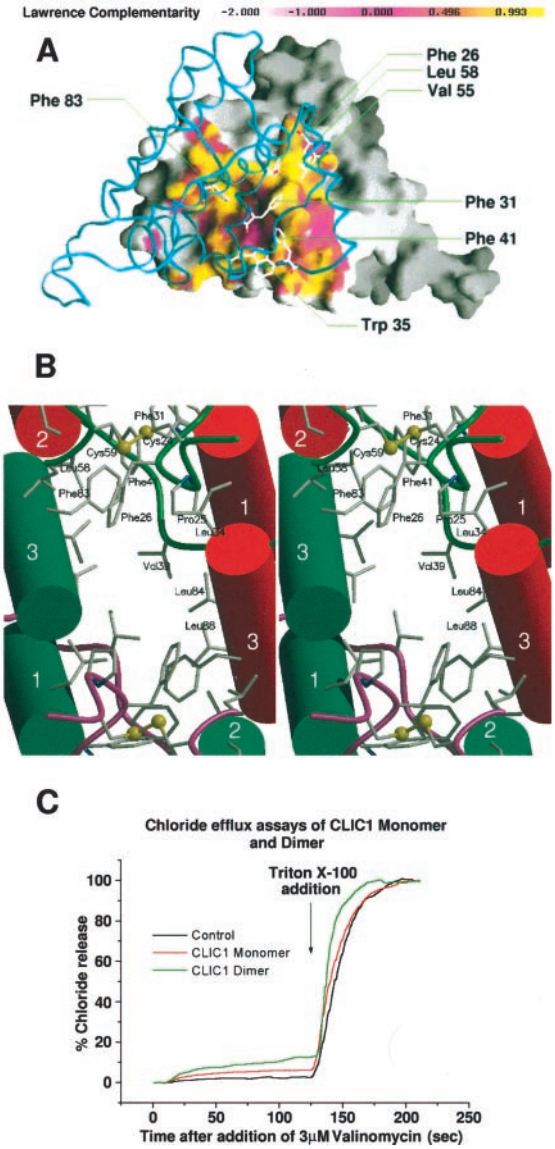

FIG. 4. **The dimer interface of oxidized CLIC1 plus channel activity.** *A*, molecular surface of the A subunit colored by Lawrence shape complementarity, S(x), of the interface (30). A backbone representation of the B subunit is displayed with residues involved in the aromatic columns labeled. The overall value for S(x) of 0.720 is comparable with oligomeric protein interfaces. The tightly packed aromatic region of the interface (*yellow*) corresponds to S(x) values close to unity, and it encloses the loosely packed inner hydrophobic region with low S(x) values (*pink*). The figure was made using GRASP (29). *B* shows a stereo view of the dimer interface. At the *top* and *bottom* of the figure are the tightly packed columns of aromatic residues, whereas there is an aliphatic cavity in the center. Helices shown as per Fig. 2. *C*, valinomycin-dependent chloride efflux from liposomes: *black line*, control; *red line*, CLIC1 monomer; *green line*, dimer. After 120 s 0.1% Triton X-100 was added to release remaining intravesicular chloride.

chloride efflux. After 2 min, Triton X-100 was added to 0.1% to release all vesicle contents.

Electrophysiology—Single-channel recordings from lipid bilayers were obtained using the tip-dip method, as previously described (10). Treated patch-clamp pipettes were dipped into a phospholipid monolayer (diphytanoyl phosphatidylcholine; Avanti Polar Lipids #850356) until pipette resistance exceeded 5 gigaohms. CLIC1 was added to the bath (final concentration of 2 μg ml^{-1}) with the same solution in both the bath and pipette (140 mM KCl, 10 mM Hepes, pH 6). Axopatch 1D and Pclamp 7 (Axon, Novato, CA) were used to record and analyze single-channel currents (recordings digitized at 5 kHz and filter at 800 Hz). Channel characterization was based on recordings that lasted more than 15 min, giving sufficient data to obtain a reproducible analysis.

TABLE II
Chloride channel activity

Protein	Cl^- Efflux[a]	Bilayer electrophysiology[b]
Control	3.7 ± 1.3% (25)	
Monomer	7.5 ± 1.5% (7)	38/56
Dimer	14.0 ± 2.7% (6)	52/72
C24S	3.8 ± 2.0% (5)	0/10 (0.001%)
C59S	3.4 ± 1.6% (5)	0/6 (0.1%)
C89S	6.7 ± 0.7% (6)	5/5 (14.5%)

[a] Chloride efflux is measured as a percentage of chloride released from the 400-nm unilamellar liposomes that occurs within 120 s after the addition of valinomycin (±S.D). Numbers in parentheses refer to the number of trials. Each set of experiments was done with protein from at least two independent preparations.

[b] The first numeral indicates the number of tip dip bilayer experiments where chloride ion channels were observed within 20 min of protein addition, and the second numeral is the total number of trials. Where no channels were observed within the experimental time, a second sample of native CLIC1 monomer was added as a positive control to ensure the integrity of the system. For the mutant proteins the number in parentheses indicates the probability (as a percentage) that the result observed would be obtained if the protein had the same properties as the wild type. The calculated probabilities assume a binomial distribution.

RESULTS

Reversible Redox-induced Dimerization of CLIC1—A feature of CLIC1 is that it possesses a glutaredoxin-like active site, suggesting that its function may be under redox control (8). To investigate this we have studied the effect of reactive oxygen species on CLIC1. Purified recombinant CLIC1 was incubated at room temperature in the presence of 2 mM hydrogen peroxide (H_2O_2) for various times and then analyzed by gel filtration chromatography. Untreated protein eluted as a monomer (Fig. 1*A*), whereas the addition of H_2O_2 resulted in the appearance of a CLIC1 dimer (Fig. 1*B*) comprising approximately two-thirds of the total protein (the proportion was unchanged between 5 min and 6 h of incubation with H_2O_2). Dimerization was completely reversed by reduction with 50 mM DTT (1 h, room temperature; Fig. 1*C*). Electrophoresis showed that the observed dimer is not primarily due to an interchain disulfide bond(s) (Fig. 1*D*), although a minor amount of such material is always present in CLIC1 samples (Fig. 1*D*, non-reducing SDS-PAGE).

Structure of the Oxidized Dimer of CLIC1—The structure of the oxidized dimeric form of CLIC1 was determined at 1.8 Å of resolution (Fig. 2; Table I). The crystal contains one dimer per asymmetric unit, with the two subunits nearly identical (root mean square deviation of 0.34 Å excluding residues 147–164). The dimer is ~75 Å long and 25 Å wide and tapers in height from 45 Å at each end to 20 Å in the middle (Fig. 2*D*). The structure is all helical, and the dimer interface occurs between the two newly configured N-domains. The arrangement of the subunits bears no relationship to that seen in GST dimers (20).

Comparison of the CLIC1 Monomer and Dimer Structures—The formation of the oxidized dimer has produced a dramatic change in the conformation of CLIC1 (Fig. 3, *A–C*). The two C-domains (residues 92–241) show only minor alterations. In contrast, the N-domain has undergone a radical structural rearrangement, including the formation of an intramolecular disulfide bond between Cys-24 and Cys-59 (Fig. 2, *B* and *C*). In the monomer, the sulfhydryl groups of these two residues are separated by 13.1 Å (Ref. 8). Cys-24 is conserved in all CLICs, where it is at the center of the glutathione-binding site in the monomeric form, whereas Cys-59 is unique to CLIC1, corresponding to a conserved Ala in all other CLICs (Fig. 2*E*).

The most apparent structural change between the monomer and dimer is the disappearance of the β-sheet (Fig. 3, *A–C*). In

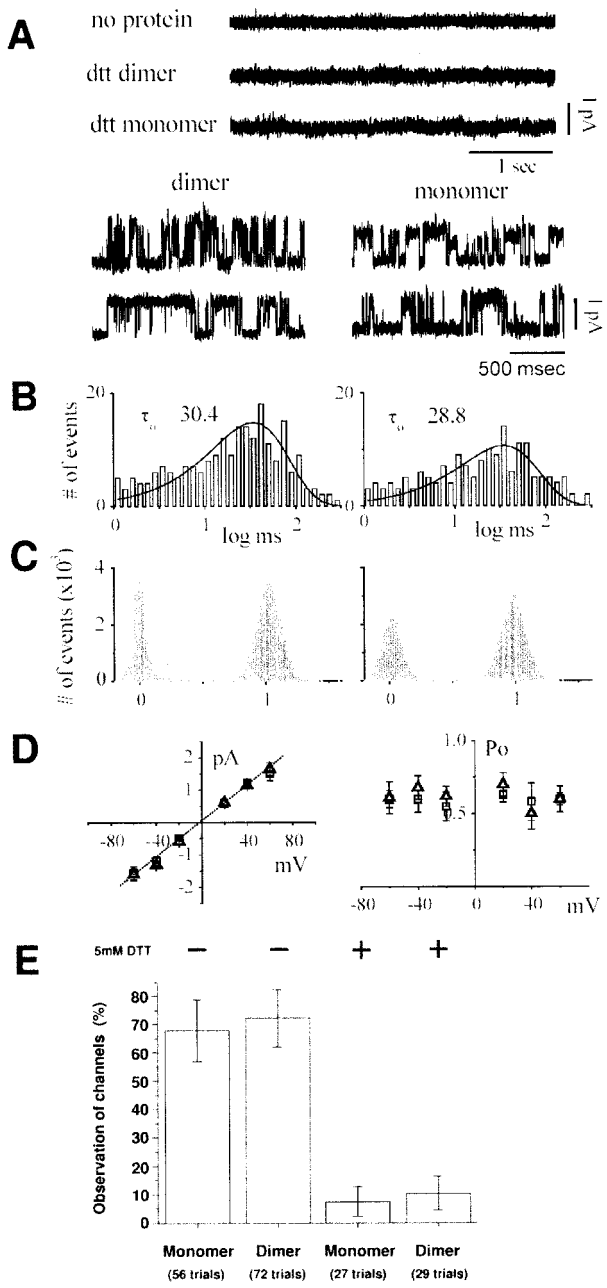

FIG. 5. **Electrophysiological characterization of the CLIC1 monomer and oxidized dimer.** *A* shows current traces from artificial bilayers all recorded at the same potential in the pipette of +30mV. The *top trace* is a control to which no protein has been added. A similar lack of channel activity was observed when either CLIC1 monomer or oxidized CLIC1 dimer were added in the presence of 5 mM DTT. The *lower panels* show typical traces (two examples each) obtained when either CLIC1 monomer or oxidized CLIC1 dimer are added under non-reducing conditions. *B*, the mean open time of the two preparations (dimer on the *left* and monomer on the *right*) obtained from 3 s of data each show similar values to those obtained previously (10). *C*, the current amplitude histograms showing the distribution of closed (*0*) and open (*1*) states obtained from 3 s of data for the dimer (*left panel*) and monomer (*right panel*). *D* shows the i/V curves (*left panel*) in which the peak amplitude histogram current values at different membrane potential are plotted for the dimer (*squares*) and for the monomer (*triangles*). The combined data can be fit to a single channel conductance of 28 ± 09 picosiemens. The *right panel* shows the open probability plot (*squares* for dimer and *triangles* for monomer), which is comparable with previous analysis (10). *E*, percentage of electrophysiological experiments (tip dip patches) where CLIC1 channel activity was observed after the addition of CLIC1 monomer or dimer ±5 mM DTT. Three different protein preparations of monomer and of dimer were used to test the effect of DTT. A null result indicates that no chloride ion channels were observed within 20 min of protein addition to a patch with a gigaohm seal. *Error bars* represent 1 S.D., computed by assuming Poisson statistics ($\sigma = \sqrt{n}$). *Numbers* in *parentheses* indicate total number of trials for each condition.

the dimer there is no electron density for the first 22 residues (β-strand 1 in monomer), and helix 2 is extended by an extra 2 turns to include residues starting at Thr-44 (originally β-strand 2; Fig. 2*E*). Residues 60–77 between helices 2 and 3 (β-strands 3 and 4 of the monomer) form an extended loop loosely packed against the C-domain in the dimer (Figs. 2*D* and 3*B*). This loop covers a tunnel filled with ordered water molecules.

Dimer Interface—The dimer interface buries ~2200 Å^2 of accessible surface (per dimer), and it is predominantly hydrophobic, consisting of two flat sheets of 4 α-helices, where each sheet comprises helices 8, 1, and 3 from one subunit and helix 2 from the other subunit (Fig. 2*C*). The interface is formed between the sheets of helices, and although the two sheets are approximately parallel, they are rotated with respect to each other by around 60° (Fig. 2*C*).

The interface can be broken into three concentric areas (Fig. 4*A*). The outermost section is lined with charged/polar residues contributed by helices 2 and 3, forming several intermolecular salt bridges. The next ring-like section consists of a tightly packed hydrophobic region dominated by two symmetry-related columns of stacked aromatic residues (Phe-83 from helix 3 slots into a hydrophobic pocket formed by Phe-26 and Phe-31 of helix 1 plus Val-55 and Leu-58 of helix 2; Fig. 4*B*). Inside this tightly packed ring there is a central hydrophobic patch composed of Leu, Ile, and Val residues contributed by helices 1 and 3. This patch is not entirely complementary across the dimer symmetry axis, resulting in an occluded cavity that is devoid of ordered water molecules (Fig. 4, *A* and *B*). Most of the hydrophobic residues at the interface are conserved within the CLIC family, except Phe-26 and Trp-35 (Ser and Leu, respectively, in CLIC3).

Monomer-Dimer Structural Transition—To understand the structural transition, the Ramachandran maps of the two structures were compared (Fig. 3, *D–F*). A Ramachandran distance was computed and plotted as a function of residue number (Fig. 2*E*). In the C-domain there are only two regions that show large Ramachandran distances. In contrast, most of the N-domain has undergone significant shifts in Ramachandran space with the exception of the residues in helices 1, 2, and 3 that are common to both structures. The major changes in the N-domain are primarily due to the transition of residues from the β-sheet region of Ramachandran space into less constrained loop structures with α-helical characteristics (Fig. 3*F*).

The Ramachandran distance plot can also be used to identify hinge regions that facilitate structural transitions. The Ramachandran distances are mapped onto backbone representations of the CLIC1 monomer and dimer structures (Fig. 3, *D* and *E*). Residues not observed in the electron density of the dimer are colored in gold on the monomer backbone trace (Fig. 3*D*). In the monomer structure most of the hinge regions reside in the N-domain, near the glutathione-binding site (*pink regions*, Fig. 3*D*).

Reduction Prevents Channel Function—To ascertain its functionality the oxidized dimer was tested for its ability to form Cl^- channels. Chloride efflux measurements from liposomes show that the dimer protein produced a significantly larger chloride flux than an equivalent concentration of monomer (Fig. 4*C* and Table II). Tip dip electrophysiological studies show that both the monomer and the dimer produce ion channels in artificial bilayers (Fig. 5) that are indistinguishable from the

channels seen in inside-out patches from Chinese hamster ovary cells transfected with CLIC1 (13). The channel characteristics for the monomer, dimer, and inside-out patches from transfected Chinese hamster ovary cells (10) are as follows: conductance, 28 ± 9, 28 ± 9, and 30 ± 2 picosiemens (Fig. 5*D*); mean open time, 28.8, 30.4, and 26.9 ms (Fig. 5*B*); open probability, 0.53 ± 0.03, 0.50 ± 0.06, and 0.53 ± 0.03 (Fig. 5*D*), respectively. All three types of channels are inhibited by IAA94.

Tip dip channel recording experiments were repeated in the presence of DTT. The probability of observing channel activity was reduced dramatically for both monomer and dimer in the presence of 5 mM DTT (Fig. 5*E*). Presumably the presence of DTT converts CLIC1 to the monomer form, which is then non-functional under reducing conditions. As a corollary of this, the channel activity observed for CLIC1 monomer is likely due to the effect of oxidation occurring in the absence of reducing agents.

Cys-24 and Cys-59 Are Essential for Dimer Formation and Channel Activity—To investigate whether disulfide bond formation is essential for channel activity the following mutant proteins were produced: C24S, C59S, and C89S. On the addition of H_2O_2 neither C24S nor C59S produced a CLIC1 dimer (Fig. 1*E*). Chloride flux measurements show that both C24S and C59S are inactive as channels, whereas C89S is indistinguishable from wild-type CLIC1 monomer (Table II). The same mutants were examined by tip dip electrophysiology. In keeping with the chloride efflux experiments channels were only observed for C89S (Table II). Statistical analysis using a binomial distribution shows that in the electrophysiological experiments C24S and C59S differ from the wild-type protein at better than the 99.9th percentile (Table II). Thus, under the conditions investigated (in particular, lipid composition) both Cys-24 and Cys-59 are essential for CLIC1 channel activity.

DISCUSSION

Our results imply that oxidation is essential for the transition of CLIC1 from the monomer to the integral membrane chloride channel form, requiring both Cys-24 and Cys-59. This suggests that the formation of the intramolecular disulfide bond between these residues is essential for the transition. The dimer structure shows that oxidation results in a large structural alteration in CLIC1 that exposes a new hydrophobic surface that is masked *in vitro* by non-covalent dimerization. *In vivo* this hydrophobic surface may represent the membrane-docking interface.

Based on these results we propose the following model for the transition between monomeric, soluble CLIC1 and the integral membrane channel form. The monomeric form maintains a GST-like structure, but the N-terminal domain occasionally transits to the conformation observed in the dimer structure. In the presence of reactive oxygen species, this altered conformation becomes trapped via the formation of the intramolecular disulfide bond between Cys-24 and Cys-59. This new, monomeric state will be unstable in solution due to the large exposed hydrophobic surface. In the presence of a lipid bilayer the conformationally altered CLIC1 monomer will dock to the membrane, whereas in the absence of lipids it will dimerize. Competition between these two processes will depend on the concentration of CLIC1 and the effective concentration of lipid bilayers. Once CLIC1 docks to the membrane it can undergo further structural changes to produce the integral membrane chloride channel form of the protein. A precedent for ion channels that are controlled by local concentrations of intracellular reactive oxygen species is the Ca^{2+} ion channel in plant root hair cells of *Arabidopsis thaliana* (21). Our working model for CLIC1 is speculative and will require further experimental verification. *In vivo* the membrane integration of CLIC1 is likely to be more complex and will probably involve other molecules.

A major unanswered question is, what is the structure of the integral membrane CLIC ion channel? Several alternative models have been proposed for the structure of the membrane inserted CLIC proteins (8, 11). Sequence analyses indicated that Cys-24 to Val-46 might form a transmembrane helix in the channel state (13). Previously, this seemed unlikely due to the GST-like monomer structure (8), which would require an unfolding of the N-domain on membrane insertion. Our present structure indicates that such an unfolding is indeed possible. However, membrane integration may also require unfolding of the C-domain (11).

The structural change observed in the monomer-to-dimer transition in CLIC1 is quite radical. Similar large scale conformational editing through redox switching has been observed in the *E. coli* H_2O_2 transcription factor, OxyR (22). Furthermore, reconciliation of biochemical evidence and the location of catalytic cysteine residues in the thioredoxin-like structure of peroxiredoxin 5 necessitate a conformational change during peroxide reduction (23). The rearrangement of the β-sheet observed for CLIC1 may, therefore, not be a unique feature of the CLIC protein family but, rather, a structural duality capable of being tolerated by the thioredoxin fold of some proteins.

REFERENCES

1. Nilius, B., and Droogmans, G. (2003) *Acta Physiol. Scand.* **177,** 119–147
2. Valenzuela, S. M., Martin, D. K., Por, S. B., Robbins, J. M., Warton, K., Bootcov, M. R., Schofield, P. R., Campbell, T. J., and Breit, S. N. (1997) *J. Biol. Chem.* **272,** 12575–12582
3. Redhead, C. R., Edelman, A. E., Brown, D., Landry, D. W., and al-Awqati, Q. (1992) *Proc. Natl. Acad. Sci. U. S. A.* **89,** 3716–3720
4. Fernandez-Salas, E., Suh, K. S., Speransky, V. V., Bowers, W. L., Levy, J. M., Adams, T., Pathak, K. R., Edwards, L. E., Hayes, D. D., Cheng, C., Steven, A. C., Weinberg, W. C., and Yuspa, S. H. (2002) *Mol. Cell. Biol.* **22,** 3610–3620
5. Schlesinger, P. H., Blair, H. C., Teitelbaum, S. L., and Edwards, J. C. (1997) *J. Biol. Chem.* **272,** 18636–18643
6. Valenzuela, S. M., Mazzanti, M., Tonini, R., Qui, M. R., Warton, K., Musgrove, E. A., Campbell, T. J., and Breit, S. N. (2000) *J. Physiol.* **529.3,** 541–552
7. Gouaux, E. (1997) *Curr. Opin. Struct. Biol.* **7,** 566–573
8. Harrop, S. J., DeMaere, M. Z., Fairlie, W. D., Reztsova, T., Valenzuela, S. M., Mazzanti, M., Tonini, R., Qiu, M. R., Jankova, L., Warton, K., Bauskin, A. R., Wu, W. M., Pankhurst, S., Campbell, T. J., Breit, S. N., and Curmi, P. M. (2001) *J. Biol. Chem.* **276,** 44993–45000
9. Dulhunty, A., Gage, P., Curtis, S., Chelvanayagam, G., and Board, P. (2001) *J. Biol. Chem.* **276,** 3319–3323
10. Warton, K., Tonini, R., Fairlie, W. D., Matthews, J. M., Valenzuela, S. M., Qiu, M. R., Wu, W. M., Pankhurst, S., Bauskin, A. R., Harrop, S. J., Campbell, T. J., Curmi, P. M., Breit, S. N., and Mazzanti, M. (2002) *J. Biol. Chem.* **277,** 26003–26011
11. Tulk, B. M., Kapadia, S., and Edwards, J. C. (2002) *Am. J. Physiol. Cell Physiol.* **282,** 1103–1112
12. Tulk, B. M., Schlesinger, P. H., Kapadia, S. A., and Edwards, J. C. (2000) *J. Biol. Chem.* **275,** 26986–26993
13. Tonini, R., Ferroni, A., Valenzuela, S. M., Warton, K., Campbell, T. J., Breit, S. N., and Mazzanti, M. (2000) *FASEB J.* **14,** 1171–1178
14. Leslie, A. (1993) *Crystallographic Computing 5: From Chemistry to Biology* (Moras, D., Pojarny, A., and Thierry, J., eds) Oxford University Press, Oxford
15. Collaborative Computing Project Number 4 (1994) *Acta Crystallogr. Sect. D* **50,** 760–763
16. Navaza, J. (1994) *Acta Crystallogr. Sect. D* **50,** 157–163
17. Lamzin, V. S., and Wilson, K. S. (1993) *Acta Crystallogr. Sect. D* **49,** 129–149
18. Jones, T. A., Zou, J. Y., Cowan, S. W., and Kjeldgaard. (1991) *Acta Crystallogr. Sect. A* **47,** 110–119
19. Murshudov, G. N., Vagin, A. A., and Dodson, E. J. (1997) *Acta Crystallogr. Sect. D* **53,** 240–255
20. Wilce, M. C., and Parker, M. W. (1994) *Biochim. Biophys. Acta* **1205,** 1–18
21. Foreman, J., Demidchik, V., Bothwell, J. H. F., Mylona, P., Miedema, H., Torres, M. A., Linstead, P., Costa, S., Brownlee, C., Jones, J. D. G., Davies, J. M., and Dolan, L. (2003) *Nature* **422,** 442–446
22. Choi, H., Kim, S., Mukhopadhyay, P., Cho, S., Woo, J., Storz, G., and Ryu, S. (2001) *Cell* **105,** 103–113
23. Declercq, J. P., Evrard, C., Clippe, A., Stricht, D. V., Bernard, A., and Knoops,

B. (2001) *J. Mol. Biol.* **311,** 751–759
24. Thompson, J. D., Higgins, D. G., and Gibson, T. J. (1994) *Nucleic Acids Res.* **22,** 4673–4680
25. Evans, S. V. (1993) *J. Mol. Graph.* **11,** 134–138
26. Kraulis, P. J. (1991) *J. Appl. Crystallogr.* **24,** 946–950
27. Merritt, E. A., and Murphy, M. E. P. (1994) *Acta Crystallogr. Sect. D* **50,** 869–873
28. Lawrence, M. C., and Bourke, P. (2000) *J. Appl. Crystallogr.* **33,** 990–991
29. Nicholls, A., Sharp, K. A., and Honig, B. (1991) *Proteins* **11,** 281–296
30. Lawrence, M. C., and Colman, P. M. (1993) *J. Mol. Biol.* **234,** 946–950
31. Laskowski, R. A., MacArthur, M. W., Moss, D. S., and Thornton, J. M. (1994) *J. Appl. Crystallogr.* **26,** 283–291

The Intracellular Chloride Ion Channel Protein CLIC1 Undergoes a Redox-controlled Structural Transition

Dene R. Littler, Stephen J. Harrop, W. Douglas Fairlie, Louise J. Brown, Greg J. Pankhurst, Susan Pankhurst, Matthew Z. DeMaere, Terence J. Campbell, Asne R. Bauskin, Raffaella Tonini, Michele Mazzanti, Samuel N. Breit and Paul M. G. Curmi

J. Biol. Chem. 2004, 279:9298-9305.
doi: 10.1074/jbc.M308444200 originally published online November 12, 2003
